Published in final edited form as:
Genes Brain Behav. 2009 July ; 8(5): 500–511. doi:10.1111/j.1601-183X.2009.00499.x.

Unidirectional startle responses and disrupted left-right coordination of motor behaviors in *robo3* mutant zebrafish

Harold A. Burgess[1], **Stephen L. Johnson**[2], and **Michael Granato**[1,*]

[1] Department of Cell and Developmental Biology, University of Pennsylvania School of Medicine, Philadelphia, PA 19104−6058

[2] Department of Genetics, Box 9232, Washington University Medical School, St. Louis, MO 63110

Abstract

The Roundabout (Robo) family of receptors and their Slit ligands play well-established roles in axonal guidance, including in humans where horizontal gaze palsy with progressive scoliosis (HGPPS) is caused by mutations in the *robo3* gene. While significant progress has been made towards understanding the mechanism by which Robo receptors establish commissural projections in the central nervous system, less is known about how these projections contribute to neural circuits mediating behavior. Here we report cloning of the zebrafish behavioral mutant *twitch twice* and show that *twitch twice* encodes *robo3*. We demonstrate that in mutant hindbrains the axons of an identified pair of neurons, the Mauthner cells, fail to cross the midline. The Mauthner neurons are essential for the startle response, and in *twitch twice*/*robo3* mutants misguidance of the Mauthner axons results in a unidirectional startle response. Moreover, we show that *twitch twice* mutants exhibit normal visual acuity but display defects in horizontal eye movements, suggesting a specific and critical role for *twitch twice*/*robo3* in sensory guided behavior.

Keywords

robo3; zebrafish; behavior; axon guidance; Mauthner cell; optokinetic response

Introduction

Bilateral symmetry is a property of the vertebrate nervous system which poses challenges for the processing of sensory stimuli and motor control. Commissural fibers play a crucial role in transferring sensory information across the midline and ensuring coordinated motor responses. During development commissural axons are initially attracted to the ventral midline, then cross to the contralateral side and are repelled from the midline. This switch in growth cone responsiveness allows growth cones to utilize intermediate targets to which they are initially attracted but then must leave to continue towards their synaptic targets (Dickson 2002; Tessier-Lavigne & Goodman 1996). DCC receptors on commissural growth cones mediate the initial attraction towards Netrin producing midline cells, while levels of Robo receptors remain low to minimize transmission of repulsive signals triggered by Slit ligands produced by midline cells (Kidd *et al.* 1998; Long *et al.* 2004). After midline crossing, growth cones express the Robo receptor, which suppresses signaling through the DCC receptor and makes the growth cone Slit responsive, thereby causing repulsion away from the midline (Kidd *et al.* 1998; Long *et al.* 2004). In the mouse, robo3 is required for axons to cross the midline (Sabatier *et al.* 2004), and analysis of alternative splice variants reveals that Robo3.1 is critical for silencing

* Email: granatom@mail.med.upenn.edu ; phone: 215−8982745 ; fax: 215−8989871.

Slit repulsion as growth cones approach the midline, while Robo3.2 acts after midline crossing with Robo1 and Robo2 to expel growth cones from the midline (Chen *et al.* 2008).

Much of our understanding of the role of Robo receptors in vertebrate neural circuit formation has been obtained from studies of commissural axon guidance. However little is known about the behavioral function of neural circuits in which commissural neurons participate. This is in part because mice lacking Robo3 die a few hours after birth, precluding behavioral tests (Sabatier *et al.* 2004). However mutations in the human ROBO3 gene cause horizontal gaze palsy with progressive scoliosis (Jen *et al.* 2004), underlining the need for animal models in which to study the neurological consequences of loss of ROBO3 function.

In a genetic screen for genes required for assembling neural circuits involved in motor behavior, we identified a small group of mutants, including *twitch twice*, with no discernable morphological phenotype but which respond to tactile or vibrational stimuli by repeatedly performing turns towards the same side (Granato *et al.* 1996). Here we report on the molecular identification of the *twitch twice* gene and show that it encodes zebrafish *robo3*. *twitch twice*/*robo3* null mutants display defects in the guidance of commissural hindbrain neurons, including the Mauthner neuron. We demonstrate that these guidance defects cause a unidirectional startle response and movement deficits specific to a subset of locomotor behaviors. Finally *twitch twice*/*robo3* mutants also exhibit specific defects in the coordination of horizontal eye movements. Thus, *twitch twice*/*robo3* mutants provide a valuable model in which to examine neurological impairments in HGPPS as well as motor behavior deficits caused by the loss of Robo3 function.

Materials and Methods

Fish Maintenance

Zebrafish (*Danio rerio*) strains used in this study were *twt*^{tw204} and *twt*^{tx209} alleles of *twitch twice*, maintained on a mixed TLF and Tubingen background. The *twt*^{tw204} and *twt*^{tx209} mutant alleles appeared to be equally penetrant and were therefore both used for anatomical and behavioral characterization. Although about 10% of homozygotes develop swim bladders, all mutants die by 14 dpf presumably as the balance and motor deficits disrupt feeding. Enhancer or gene trap j1229a that expresses GFP in reticulospinal neurons including the Mauthner cells was identified in an enhancer/gene trap screen. The tol2 gene trap plasmid T2KSAG (Kawakami *et al.* 2004) was coinjected with tol2 transposase mRNA. Embryos with any GFP positive cells were reared to adult stages and their progeny were screened for specific expression patterns. Single insert lines were obtained by multiple generations of outcrossing and monitored by Q-RT-PCR. Once a single insert line was established, we used Tail-PCR (Parinov *et al.* 1999) to identify the genomic insertion site, at chr11:9,246,478 bp (ZV7 assembly). This location was confirmed by co-segregation of the reticulospinal expression pattern with PCR-based markers specific to the transposon in its insertion site (see http://www.genetics.wustl.edu/fish_lab/tol2/alleles/j1229a/j1229a.html). The j1229a insertion is not in or near an obvious gene, and thus, the underlying molecular basis for its reticulospinal expression pattern is obscure.

Embryos were collected in the morning and thereafter maintained on a 14/10 hour light/dark cycle at 28°C unless otherwise noted. Larvae were raised in 6 cm plastic Petri dishes at a density of 20−30 per 7 mL in E3 medium (5 mM NaCl, 0.17m mM KCl, 0.33 mM $CaCl_2$, 0.33 mM $MgSO_4$) with medium changes at 2 dpf (days post fertilization) and 4 dpf. Behavioral experiments were conducted on 5−7 dpf.

Recombination Mapping and Molecular Cloning

A three generation mapping cross between *twt*^{tw204} heterozygous and WIK fish was generated, and pools of 25 F_2 mutant and 25 F_2 sibling larvae were collected in the F_2 generation and used for bulk segregant mapping. Mutant larvae were identified by visible abnormalities in the behavioral response to an acoustic or tactile startle stimulus, with larvae repeatedly bending to the same side, losing rhythmic left-right alternating tail movements (Granato *et al.* 1996) and failing to retain an upright posture throughout the response (see Results). For identifying the mutation, Robo3 cDNA was amplified in two fragments from 5 or 6 dpf larvae by RT-PCR, with primer design using Primer3 (Rozen & Skaletsky 2000). RT-PCR was carried out using the Access RT-PCR kit (Promega, Madison, WI) with 70 pmol of each primer and 500 ng of total mRNA prepared using TRIzol Reagent (Invitrogen, Carlsbad, CA) according to the manufacturer's protocol. For 5−6 dpf larvae, we used 20 μL TRIzol per larva. Control reactions containing no RNA or no reverse transcriptase were also performed. The primers for the 5' fragment were 5'-TTTAGGGGACTGTTTGTCCG and 5'-AATCTCGTACTCGGTGCCTTT and the primers for the 3' fragment were 5-GTCGCAGTACATCCAGGGTT and 5'-TTCCGAATGAAAACAGAGGG. RT-PCR conditions were 48 °C for 45 min; 94 °C for 2 min; and then 5 cycles of 94 °C for 45 s, touchdown at 60 °C to 55 °C for 45 s, and 68 °C for 150 s; and then 40 cycles of 94 °C for 45 s, 55 °C for 45 s, and 68 °C for 150 s. Products were gel-purified and cloned into pGEM-T Easy (Promega, Madison, WI) for sequencing. After comparing sequence derived from fragments cloned from mutant and sibling larvae, mutations were verified by repeating the RT-PCR on fresh pools of mutant and sibling larvae and directly sequencing gel-purified cDNA. All nucleotide numbers for *robo3* refer to the Genbank mRNA sequence AF337036 (Robo3var1).

PCR Genotyping Twitch twice

We developed a dCAPS assay (Neff *et al.* 2002) using the dCAPS program (http://helix.wustl.edu/dcaps/dcaps.html) for genotyping both *twitch twice* alleles. For genotyping the *twt*^{tx209} allele (C583T mutation) the primer pair is 5'-GAGCCTGCAACTTTGAACTG and 5'-CACACGTACACGCCTTCATC. PCR is performed using 0.5 μM primers in RAPD buffer, using conditions: 94°C for 3 min then 3 cycles of 94°C for 45 s, touchdown 60 °C to 57 °C for 45s, 72 °C for 15s, then 37 cycles of 94 °C for 45s, 57°C for 45s, 72 °C for 15s. The PCR product is then digested with FokI. The wildtype allele remains uncleaved at 194 bp, while the mutant allele is digested producing a 160 bp fragment which can be distinguished on a 3% agarose gel containing 2% Metaphor agarose (Lonza, Rockland, ME). For genotyping the *twt*^{tw204} allele (TC2099AA mutation), the primer pair is 5'-TGGTGGTCTATCAGCATCTCC and 5'-CGGAGATGTTTGCTGTGTAGTT. PCR is performed as above and the product is digested with Eco57I. The wildtype allele is cleaved and contains a 160 bp fragment, while the mutant allele remains uncut at 194 bp. This protocol was used both for genotyping *twitch twice* adults and for genotyping larvae before the behavioral phenotype is manifest at 5 dpf.

Immunohistochemistry

To produce anti-Robo3 antisera, we subcloned a fragment of the *robo3* cDNA encoding a 125 amino acid peptide predicted to be part of the Robo3 intracellular domain (amino acids 1142 to 1267, see Figure 1C) into the PRSET vector (Invitrogen, Carlsbad, CA) in frame with a 6HIS tag. This was transformed in BL21DE3RIL bacteria (Stratagene, La Jolla, CA) and protein expression was induced with 1.0 mM IPTG. Bacteria were pelleted and resuspended in 10 mM Tris pH 8.0, 100 mM NaH_2PO_4, 8M Urea for lysis. Tagged protein was then purified on a NiNTA column using the manufacturer's denaturing protocol. Fractions containing the expressed protein were dialyzed into 4M Urea. These were then sent for immunization into rabbits (Prosci Inc, Poway, CA). Bleeds were tested using wholemount immunostaining and

western blot from protein extracts of 24 hpf larvae. One bleed showed faint signs of reactivity, but high background. We therefore coupled the 6HIS tagged peptide to an Affigel-10 (BioRad, Hercules, CA) immunoaffinity column using the manufacturer's protocol and absorbed the antisera to the column. We eluted with 0.1 M glycine pH 2.5 and pooled the most concentrated fractions for immunostaining. Purified anti-Robo3 was diluted 1:100 in PBS and pre-absorbed to fixed embryos at 4°C overnight. For immunostaining, 10% normal goat serum and 0.5% Triton X-100 were added pre-absorbed antibody. Larvae were for 3 hours at 4 °C in 4% paraformaldehyde with 1% DMSO, treated with 1 mg/mL collagenase for 6 minutes and blocked for 30 minutes with 10% fetal bovine serum in PBS. Other antibodies used were GFP JL-8 (1:100 dilution, Clontech, Mountain View, CA) and 3A10 (1:50, (Hatta 1992), kind gift of Dr. T. Jessell). Primary antibodies were detected by AlexaFluor488 or AlexaFluor594 conjugated secondary antibodies (1:200, Invitrogen, Carlsbad, CA) or biotinylated anti-mouse antibody with the color reaction performed using the Vectorstain ABC kit (Vector Laboratories, Burlingame, CA). Images were acquired with a Leica LCS confocal microscope and a Zeiss Axioplan microscope.

Behavioral Assays

All behavioral measurements were made with the *Flote* software package (Burgess & Granato 2007a; b). Briefly, this software performs tracking of larvae filmed in groups of up to 30 larvae, then performs automated analysis of body curvature on each larva to extract kinematic details of swimming movements. Discrete locomotor movements are identified using kinematic features. In all experiments, larvae were pre-adapted to the intensity of light in the testing arena for at least 3 hours. Video recordings were initiated 2 minutes after moving larvae to the testing arena in order to allow sufficient time for locomotor activity to stabilize (Burgess & Granato 2007a). All video recordings were made with a Motionpro high speed camera (Redlake, Tucson, AZ) 512×512 pixel resolution, using a 50 mm macro lens at 1000 frames per second unless otherwise noted. Experiments were carried out at 26−28°C.

Behavioral analysis of *twitch twice* larvae is complicated by the frequency with which they fail to assume a vertical orientation in the water, instead falling toward one side. When filmed from above, the initial flexion of the body is therefore toward or away from the camera, not detectable with this recording configuration. However, larvae which fail to maintain a vertical orientation show only a single eye to the camera (Fig. 4a), allowing us to exclude these larvae from analysis. In addition, larvae already engaged in locomotion at the beginning of a video recording were excluded from analysis, as were larvae initiating movement in the last 20 ms, as insufficient frames remain to determine the typed of motor pattern being initiated.

Stationary balance was measured by taking a one minute video (1 frame/s), with illumination provided by an array of 80 infrared LEDs (940 nm peak; ILED-8, AllElectronics, Van Nuys, CA), mounted 75 mm below the testing arena. A dorsally positioned light was provided (300 μW/cm2) although it is not clear that young larvae actually use this information for vertical orientation. Larvae with balance deficits were detected by their horizontal posture as described above. For each group, the percentage of observations of larvae with a horizontal posture was calculated.

Dark Flash responses were measured by pre-adapting larvae to 300μW/cm^2 white light before moving them to the testing arena. In the testing arena, illumination was provided by an array of six white LEDs (Jameco Electronics, 320531, Belmont, CA) adjusted to 300μW/cm^2 using GamColor neutral density filters (GAM, Los Angeles, CA) and controlled by a Stamp BS2sx microcontroller (Parallax, Rocklin, CA, USA). The microcontroller simultaneously triggered the camera to start recording a 1000 frame burst coincident with turning the light off for 1 second (a ‘dark flash’). Larvae were tested in groups of 20 per plate, with each group subjected to a series of 8 dark flashes presented at 1 minute intervals.

Startle responses were elicited using either of two techniques. To measure startle responsiveness, kinematics and balance, larvae were tested in groups of 20, using a small vibration exciter (4810, Bruel and Kjaer, Norcross, GA), controlled by an digital-analogue card (PCI-6221, National Instruments, Austin, TX) which also triggered the camera to collect a 120 frame (120 ms) window. All startle stimuli were 3 ms duration 1000 Hz waveforms, of variable intensity as specified in the text, generated by custom software. *Bend angle, duration* and *maximal angular velocity* are as previously defined (Burgess & Granato 2007a). *Locomotor balance* was measured by tracking the position of the eyes for each larva during every frame of its response to the stimulus. Wildtype larvae remain vertically oriented for at least 90% of frames even during the vigorous movements made in response to startle stimuli. Thus responses are scored as balanced only if both eyes can be identified in >90% of frames. In experiments in which startle directionality was assessed, an impact 'tap' stimulus was delivered by a tubular solenoid (S-63−38-H, Magnetic Sensor Systems, Van Nuys, CA), whose activation was coordinated with the video camera using a Stamp microcontroller. Startle inducing stimuli were delivered at 15 second intervals to minimize habituation. We excluded larvae which were horizontally oriented at the beginning of the recording window from further analysis as these larvae tend to lie against the bottom of the dish may receive a tactile stimulus in addition to the acoustic stimulus. In addition we cannot effectively analyze kinematics or direction of movement in these larvae.

Optokinetic responses were elicited using a DLP projector (PG-M20x, Sharp, Mahwah, NJ) following the protocol of Huang and Neuhauss (Huang & Neuhauss 2008). Larvae were embedded in 50 μL of 3% methylcellulose on a 3 cm Petri dish with one eye facing a cylindrical diffusion screen at a distance of 12 cm and the other eye facing a black piece of paper. Illumination was provided with an infra-red array as described above. Using the DLP projector, a vertical step grating (0.053 cycles/° spatial frequency) was moved in either a nasal to temporal direction, or the reverse, at a constant velocity of either 8.3 °/s or 16.7 °/s for 4 seconds. The grating was corrected for the curvature of screen so that the spatial frequency remained constant across the screen. The intensity of the grating stepped from 115 $\mu W/cm^2$ to 0.34 $\mu W/cm^2$. Each larva was presented with 3 stimuli for each combination of direction and velocity (12 trials total). Software for the stimulus was written in IDL (ITT Visual Information Solutions, Boulder, CO). Video recordings were made at 100 fps, with the start synchronized to the initiation of the test using a microcontroller and a photodiode. Code for analysis of eye velocity was written in IDL. First a bandpass filter was applied and local maxima in the field (corresponding to eye centroids) found. Pixels of similar intensity to the centroid were located and their position used as input to the Fit_Ellipse routine (courtesy of David Fanning, www.dfanning.com) to find the orientation of the major axis of the fitted ellipse. The orientation time series was smoothed using a boxcar function (width 21 points) and the angular velocity of eye rotations was measured by finding the gradient of the linear fit to the interval between the end of the first second of stimulation and the first saccade (if any). Optokinetic gain was calculated as the ratio of the angular velocity of eye movement to the angular velocity of the stimulus. The relatively low gains reported here are consistent with results derived by other groups using monocular stimulation in larval zebrafish (Beck *et al.* 2004 ; Qian *et al.* 2005). Circuit diagrams and software will be provided upon request.

Statistical Analyses

All statistical analysis was performed using SPSS 14.0 (SPSS, Chicago, IL, USA). Where appropriate, P values were subjected to Bonferroni correction to maintain alpha of 0.05. Graphs show mean and standard error except where otherwise noted.

Results

Molecular cloning of *twitch twice*

Using recombination mapping, we mapped the *twitch twice* locus to a 1.7 cM interval between two simple sequence length polymorphic markers, z531 (4/254 recombinants) and z9574 (6/248 recombinants) on chromosome 10 (Fig. 1a). Several mRNAs and ESTs had previously been mapped to this interval, including Robo3. Sequencing of *robo3* cDNAs isolated from *twt*^{tw204} mutant larvae revealed two adjacent nucleotide changes, T2099A and C2100A, introducing a premature stop codon predicted to truncate the protein in the first fibronectin repeat of the extracellular domain (Fig. 1b,c). We then amplified and sequenced cDNAs from the *twt*^{tx209} allele and found a C583T nonsense mutation, predicted to truncate Robo3 in the first immunoglobin repeat at amino acid 58, thereby generating a presumptive null allele (Fig. 1b,c). Thus, sequence analysis identified premature stop codons in two independent *twitch twice* alleles, demonstrating that the *twitch twice* phenotype is caused by mutations in the *robo3* gene.

Mauthner cell pathfinding defects in *twitch twice*/*robo3*

Previous studies demonstrated that zebrafish Robo3 is expressed in regions of the hindbrain consistent with the position of differentiating reticulospinal neurons (Challa *et al.* 2001; Lee *et al.* 2001); (Challa *et al.* 2005). In mice lacking Robo3, commissural spinal cord and hindbrain axons fail to cross the midline because they become prematurely Slit responsive (Sabatier *et al.* 2004). To determine the role of *twitch twice*/*robo3* in zebrafish midline guidance, we examined the axonal trajectory of identified hindbrain neurons, the Mauthner cells, a pair of large reticulospinal neurons which project to the contralateral spinal cord starting at 17 hpf (Fig. 2a). Immunohistochemistry with the 3A10 antibody revealed a dramatic Mauthner cell pathfinding defect in a subset of mutants. In these larvae, one Mauthner axon, instead of traversing the ventral midline, projects ipsilaterally to the spinal cord (Fig. 2b). In rare instances, both Mauthner axons project ipsilaterally to the spinal cord (Fig. 2c). No instances of Mauthner pathfinding defects were observed in wildtype sibling larvae (n=312). The Mauthner pathfinding defect in *twitch twice*/*robo3* mutants is temperature sensitive, with 48% (73/153) of the larvae displaying the phenotype when raised at 22°C for the first 24 hours post fertilization, dropping to 19% (13/68) when raised at 28°C over the same period (Fisher's exact test $p<0.001$). At 24°C, 37.3% of larvae have a single Mauthner axon defect and 10.5% have a double ipsilateral projection, consistent with the probability of a misprojection being independent for the two cells. Commissural pathfinding defects are not restricted to Mauthner axons. In wildtype sibling larvae, the 3A10 antibody reveals a ladder of seven commissural tracts in the caudal hindbrain (Lorent *et al.* 2001) (Fig. 2d). In *twitch twice/robo3* larvae, the hindbrain commissures are disorganized, defasciculated and frequently merge. However, unlike in *space cadet* mutants (Lorent *et al.* 2001), the morphology of the axon cap is normal (Fig. 2e).

robo3 Expression in Commissural Axons

To examine the expression of Robo3 protein as commissural axons cross the midline, we raised polyclonal antibodies against zebrafish Robo3. Immunohistochemical staining with this antibody reveals a ladder of commissures in the hindbrain of 48 hpf wildtype sibling larvae (Fig. 3a). Commissure staining is absent in *twitch twice* mutants, demonstrating the specificity of the antibody for Robo3 (Fig. 3b). Next we examined wildtype larvae at 18 hpf, when Mauthner axons approach the ventral midline. In order to identify Mauthner axons, we used a transgenic line with early GFP expression in the Mauthner cell (Miyashita *et al.* 2004). Double staining with anti-GFP and anti-Robo3 antibodies revealed accumulation of Robo3 protein on the growth cones of Mauthner cells before they reached the ventral midline (Fig. 3c). This is consistent with the role of Robo3 in mouse, where expression on pre-crossing commissural

axons renders them insensitive to Slit, thereby enabling these growth cones to approach and cross the ventral midline .

Startle responses in *twitch twice*/*robo3* mutant larvae

In fish the Mauthner cell plays a central role in controlling startle responses (Eaton *et al.* 1981 ; Kimmel *et al.* 1980 ; Liu & Fetcho 1999). We therefore examined the startle response in *twitch twice*/*robo3* mutant larvae. We noticed that whereas normal larvae remain vertically oriented in the water column, *twitch twice*/*robo3* larvae often lay on their side at the bottom of the dish when stationary and frequently rolled over during the startle response, suggesting a balance impairment (Fig. 4a). Measurement of this phenotype demonstrated that mutant larvae show a significantly higher incidence of poor balance in the absence of stimulation (n=5 groups each genotype, t-test p=0.006 ; Fig. 4b). Wildtype sibling larvae maintain a vertical posture throughout the startle response (supplementary movie 1a). In contrast, mutant larvae roll during the course of the response (supplementary movie 1b). As wildtype larvae occasionally tilt briefly during the startle response, we set a threshold for normal responses as being those where the fish remained upright for more than 90% of the frames analyzed. Based on this criterion, 94.6% ± 0.4% of wildtype sibling startle responses were upright, compared to only 55.6% ± 1.7% of mutant startles (n=5 groups per phenotype, t-test p=0.003 ; Fig. 4c). Wildtype larvae respond to a sudden decrease in illumination (‘Dark Flash’) by performing a slow turn in which the head and tail of the larvae almost touch (‘O-bend’), followed by a counterbend and bout of swimming (Burgess & Granato 2007a). Mutants are also unstable during responses to Dark Flash stimuli with only 68.5% ± 6.9% of mutant O-bends maintaining an upright posture compared to 96.2% ± 1.9% of responses in wildtype siblings (n=5 groups per phenotype, t-test p=0.01). Thus *twitch twice/robo3* larvae have impaired balance, leading to abnormal rolling during vigorous locomotor responses.

We have previously shown that zebrafish larvae show two stereotyped modes of response to acoustic startle stimuli (Burgess & Granato 2007b). One mode of response occurs at very short latency to the stimulus (less than 15 ms) and is initiated with an explosive C-bend of the body (short latency C-start or ‘SLC’ response). The second type of response occurs at a longer latency (mean 28 ms) and has less vigorous kinematic properties (long latency C-start or ‘LLC’ response). Moreover, SLC responses are the classic Mauthner mediated startle response of teleost fish, while LLC responses are Mauthner independent. To determine whether SLC and/or LLC behavior depend on the neural circuitry established by Robo3 guidance, we tested responsiveness to acoustic/vibrational stimuli. *twitch twice*/*robo3* mutants showed almost identical SLC responsiveness when compared to wildtype sibling larvae (two-way ANOVA, no effect of genotype F[1,16]=2.1, p=0.16 ; Fig. 4d). However, mutants showed a quantitative reduction in LLC responsiveness (two-way ANOVA, main effect of genotype F[1,16]=7.9, p=0.012 ; Fig. 4e). LLC responses are mediated by the otoliths of the inner ear, and are also required for balance. Otoliths are normal in *twitch twice/robo3* fish, thus the impairment in both balance and LLC responsiveness suggests that stato-acoustic afferents are impaired in *twitch twice/robo3*.

In *twitch twice*/*robo3* mutants, one of the two Mauthner axons frequently fails to cross the midline and instead projects to the ipsilateral side to the spinal cord. Thus, one side of the spinal cord receives a double innervation of Mauthner axons, while the other side receives no such input. We therefore hypothesized that in such single ipsilateral *twitch twice* mutants, SLC responses should be selectively lateralized. To test this, we first sorted larvae according to their Mauthner cell phenotype, using the 1229a enhancer trap line with GFP expression in 4 dpf Mauthner cells and axons (data not shown). Individual larvae were then tested with a series of acoustic/vibrational stimuli delivered to the side of the Petri dish by a solenoid (Burgess & Granato 2007b). Wildtype larvae and *twitch twice*/*robo3* mutants in which both Mauthner

axons crossed the midline showed no directional bias to SLC responses with close to 50% of responses being made in a rightward direction (Fig. 4f). In contrast, *twitch twice*/*robo3* mutants in which the left Mauthner axon projected together with the right Mauthner axon to the left spinal cord, showed almost exclusively leftward SLC responses (3.3±1.7% of responses were rightward, one sample t-test versus 50%, $p<0.001$). Similarly, in mutants where the right Mauthner axon projected ipsilaterally, SLC responses were almost entirely rightward (98.6 ± 1.4% of responses rightward, one-sample t-test versus 50%, $p<0.001$). In the rare mutants where both Mauthner axons failed to cross, SLC responses showed no directional bias, reflecting the fact that both sides of the spinal cord received Mauthner innervation. Confirming our previous data showing that LLC responses do not require the Mauthner cell, these responses were initiated leftward and rightward with equal frequency in all groups (Fig. 4g). Thus miswiring of the neural circuit mediating startle responses in *twitch twice*/*robo3* mutants specifically impairs the ability of the fish to generate SLC responses in both left and right directions.

Kinematic Defects in *twitch twice*/*robo3*

To examine in more detail the behavioral defects observed in *twitch twice*/*robo3* mutants, we analyzed the kinematic properties of the first C-bend and counterbend of responses made to acoustic and visual stimuli (Table 1). The kinematic properties of SLC startle responses made by *twitch twice*/*robo3* mutants to acoustic stimuli were indistinguishable from wildtype sibling larvae (Fig. 5a, Table 1). In contrast LLC responses to acoustic startle stimuli were characterized by an extended duration of the first C-bend and reduced angular velocity of the counter-bend such that larvae appear to perform a single ‘twitch’ in response to the stimulus (Fig. 5b ; Table 1). Mutant larvae show similar responsiveness to Dark Flash stimuli (siblings 93.2% ± 2.7%, mutants 84.8% ± 3.5% ; n=5 groups each ; t-test $p=0.092$). However O-bend responses to Dark Flash stimuli were affected in a similar fashion to LLC responses in that the duration of the initial C-bend was greatly extended and the counter-bend performed at reduced angular velocity (Fig. 5c ; Table 1). In addition, the angular velocity of the initial C-bend was reduced. As for LLC responses, the effect was to produce a ‘twitch’ response to the stimulus (supplementary movie 2a and 2b). The lack of an impairment in the kinematics of SLC responses suggests that muscle function is not impaired in mutants and that ‘long slow’ kinematics of LLC and O-bend responses reflect deficits in neural circuits generating these responses.

Failure to Coordinate Horizontal Eye Movements in *twitch twice*/*robo3*

The *ROBO3* gene has been implicated in the human neurological disorder horizontal gaze palsy with progressive scoliosis (Jen *et al.* 2004). In HGPPS, patients show a near complete absence of all horizontal gaze reflexes (Bosley *et al.* 2005). We therefore asked whether zebrafish *robo3* mutants recapitulated this phenotype. Horizontal eye movements can be evoked in zebrafish larvae by eliciting the optokinetic response (OKR) to a horizontally moving grating (Fig. 6a) (Clark 1981; Easter & Nicola 1997).

First, we tested the response of the eye facing the optokinetic stimulus. When tested with a moving grating moving from the temporal to nasal direction *twitch twice*/*robo3* mutants and siblings showed an almost identical ability to track the grating under both low and high angular velocity stimulus conditions (two-way ANOVA, no effect of genotype $F_{[1,56]}=0.22$, $p=0.64$; main effect of stimulus velocity $F_{[1,56]}=4.3$, $p=0.044$; Fig. 6b). Thus, similar to the situation in HGPPS patients, horizontal eye movements are not overly impaired in zebrafish *robo3* mutants. Lateral eyed, afoveate animals including zebrafish less effectively track stimuli moving in the nasal to temporal (NT) direction (Qian *et al.* 2005;Roeser & Baier 2003). Consistent with this, we found that in wildtype sibling fish the optokinetic gain for NT stimuli was reduced by 50% when compared to temporal to nasal stimulation. In contrast, gain was

reduced by almost 90% in *twitch twice*/*robo3* mutants such that mutants showed a significantly lower gain than siblings for NT stimuli (main effect of genotype, $F_{[1,56]}=55.7$, $p<0.001$; Fig. 6b).

Next we examined movements of the unstimulated eye during the OKR. Stimulation of one eye during the optokinetic response triggers lower gain but same-direction movements by the unstimulated eye (Qian *et al.* 2005 ; Rinner *et al.* 2005). We found that coordinated rotation of the unstimulated eye was greatly reduced in mutants compared to sibling larvae (ANOVA, main effect of genotype $F_{[1,56]}=10.9$, $p=0.002$; Fig. 6c). As the stimulated eye has a normal OKR response, it is unlikely that *twitch twice/robo3* has reduced visual acuity or a motor deficit. Rather, the poor response of the unstimulated eye likely represents a failure to transmit signals for motor control to the opposite side of the brain.

Discussion

Here we demonstrate that two alleles of the *twitch twice* mutant contain nonsense mutations in the *robo3* gene. One allele of *twitch twice*/*robo3* harbors a rare double mutation in neighboring base pairs. While ENU usually induces single nucleotide mutations, changes in adjacent base pairs have been reported (Douglas *et al.* 1995). Mutations in both alleles are predicted to truncate Robo3 in the extracellular domain thereby acting as null alleles. We show that *robo3* is required for midline guidance of commissural axons in zebrafish and demonstrate that miswiring of Mauthner cell projections leads to unidirectional initiation of the startle response and defects in the coordinated expression of other motor behaviors.

As in mammals, four Robo receptors have been identified in zebrafish (Challa *et al.* 2001; Lee *et al.* 2001; Park *et al.* 2003). The zebrafish *robo2/astray* gene is critical for guidance of retinal ganglion cell and olfactory axons (Fricke *et al.* 2001; Miyasaka *et al.* 2005). Both N-terminal and C-terminal alternative splice variants of the mouse *robo3* gene have been described, with amino terminal splice products showing differential Slit binding (Camurri *et al.* 2005 ; Chen *et al.* 2008; Mambetisaeva *et al.* 2005 ; Sabatier *et al.* 2004). Similarly, the zebrafish *robo3* gene produces two isoforms which vary in their amino termini. Robo3var1 is predominantly expressed in non-neuronal cells (somites, fin bud mesenchyme) and morpholino mediated knockdown of Robo3var1 causes defects in dorso-ventral pattering of the early embryo (Challa *et al.* 2005). Robo3var2 is more restricted to neural tissues (hindbrain, spinal cord) (Challa *et al.* 2005). The mutations in *twitch twice* affect both Robo3var1 and Robo3var2, however maternal transcripts of *robo3* are present in zebrafish (Challa *et al.* 2005) ; Burgess and Granato, data not shown), and may compensate for the loss of zygotic protein, explaining the partial penetrance of the Mauthner axon decussation defect in *twitch twice/robo3* mutants.

Robo3 is a divergent member of the Robo family (Challa *et al.* 2001; Lee *et al.* 2001) which shares only partial sequence conservation of the CC1 and CC2 motifs, necessary for signaling via DCC and Ena (Bashaw *et al.* 2000; Stein & Tessier-Lavigne 2001). The Drosophila Robo2 protein which also lacks the CC2 motif, appears to mediate a weaker response to midline Slit and through heterodimerization, may inhibit Robo signaling (Rajagopalan *et al.* 2000; Simpson *et al.* 2000). This suggests that zebrafish *Robo3* may also function to block signaling through Robo to facilitate commissural axon extension toward the midline despite the presence of Slit. Consistent with this, we find that Robo3 protein is expressed on the growth cones of Mauthner cells extending toward the ventral midline. Similarly, in the mouse, the Robo3.1 isoform is expressed and functions as commissural axons approach and cross the midline to antagonize midline Slit repulsion (Chen *et al.* 2008).

In humans, mutations in the ROBO3 gene cause horizontal gaze palsy with progressive scoliosis. While we did not observe scoliosis in young larvae, this likely reflects the relatively

late onset and progressive nature of scoliosis in patients (Bosley *et al.* 2005; Dretakis & Kondoyannis 1974). It was not possible to examine older animals as homozygous mutant fish die by 14 dpf. Although the neurological basis of horizontal gaze palsy in HGPPS remains unclear, patients show a loss of brainstem commissural tracts and midline crossing defects in long ascending medial lemniscal and descending corticospinal tracts (Bosley *et al.* 2005 ; Sicotte *et al.* 2006). In consequence ipsilateral motor cortex is activated during motor tasks where contralateral activation is seen in normals (Haller *et al.* 2008). Our finding that *robo3* mutations also cause commissural fiber defects in *twitch twice* represents an opportunity to analyze circuit level defects that contribute to the neuropathology of this disorder.

Behavioral deficits in *twitch twice/robo3* mutants do not reflect simple deficits in sensory acuity or motor function as fish show normal levels of sensitivity to acoustic and visual stimuli and the initial C-bend and counterbend of SLC startle responses are similar to wildtype. Rather, consistent with an essential role for commissural tracts in distributing sensory information to the two sides of the nervous system and facilitating coordinated motor output, we found that *twitch twice/robo3* mutants show subtle behavioral defects in coordinating left and right motor responses to stimuli.

The most dramatic phenotype of *twitch twice/robo3* larvae is the unidirectional initiation of short latency startle responses to acoustic stimuli in the subset of mutants with a unilateral Mauthner axon midline crossing defect. The teleost Mauthner cell has long been implicated in mediating startle responses (Kimmel *et al.* 1980 ; Liu & Fetcho 1999; Yasargil & Diamond 1968 ; Zottoli *et al.* 1999). Zebrafish larvae exhibit two distinct modes of response to an acoustic startle stimulus, a Mauthner-mediated explosive response initiated at short latency to the stimulus (SLC) and a long latency, less vigorous non-Mauthner response (LLC) (Burgess & Granato 2007b). In mutants in which one Mauthner cell fails to cross the midline, instead projecting with the other Mauthner cell to the ipsilateral spinal cord, SLC responses are initiated in one direction only while LLC responses remain bidirectional. As *twitch twice/robo3* larvae show a significant balance defect, we suspect that the rare instances in which responses are made to the side receiving no Mauthner input simply represent larvae positioned upside-down, a posture which can not be detected in our images. *Robo3* therefore plays a key role in ensuring that the neural circuit mediating the startle response is able to trigger SLC movements in both directions.

While the kinematics of SLC responses of mutant larvae are indistinguishable from wildtype siblings, we find that other types of stereotyped movement are impaired. The initial C-bend and counterbend of LLC responses to acoustic stimuli and O-bend responses to Dark Flash stimuli have reduced angular velocity and extended response duration. This resembles a weak ‘accordion’ phenotype characterized by defects in the normal alternation of contraction of the two sides of the tail musculature. In the *bandoneon* mutant, a mutation in the glycine receptor β-subunit disrupts reciprocal inhibition required to coordinate this process (Hirata *et al.* 2005). The kinematic defects in *twitch twice/robo3* could therefore reflect a degradation in reciprocal inhibition at the spinal level, or alternatively arise as a result of inappropriate bilateral activation of hindbrain locomotor circuits. Indeed Robo3 is expressed in both locations. However as SLC responses are spared in mutants, we suspect that the locomotor phenotype reflects disrupted communication between the two halves of the brainstem resulting in bilateral activation of response movements. This may correspond to the intriguing finding that in HGPPS patients, left-sided monaural stimulation triggers bilateral activation of the primary auditory cortex rather than activation only of the contralateral side (Haller *et al.* 2008). The fact that SLC responses do not show signs of bilateral activation may be a peculiarity of the escape circuitry which safeguards against simultaneous activation of both sides of the tail musculature by the two Mauthner cells during urgent escape responses (Faber & Korn 1978).

As the most pronounced neurological deficit in HGPPS is the near complete absence of horizontal gaze reflexes, we measured the optokinetic reflex to a horizontally moving grating in *twitch twice/robo3* larvae. Optokinetic defects have been described in a variety of zebrafish mutants, including the *belladonna* mutant in which retinal ganglion cell axons fail to cross the midline and project to the ipsilateral brain (Rick *et al.* 2000). Achiasmatic mutants show reversed optokinetic responses, thought to reflect ipsilateral target regions incorrectly interpreting the stimulus as having the reverse direction and driving compensatory eye movements accordingly. In contrast, in *twitch twice* retinal ganglion cell axons successfully decussate at the optic chiasm (data not shown), thus input to the central optokinetic system is likely normal, and indeed we did not find a significant difference in optokinetic gain when the stimulated eye was presented with a TN directed stimulus. Surprisingly though, *twitch twice/robo3* larvae show a markedly reduced response to optokinetic stimuli moving in the NT direction.

In frontal eyed, foveate animals, the optokinetic response is primarily mediated by the cortex, with rapid eye movements in both TN and NT directions serving to maintain stability of the target image on the fovea (Harris *et al.* 1980). However in lateral eyed, afoveate animals like fish, optokinetic movements are produced by brainstem regions homologous to the nucleus of the optic tract (NOT) and are less efficient at tracking NT directed stimuli (reviewed in (Huang & Neuhauss 2008)). Evidence from mammals suggests that each NOT is activated by TN directional stimuli at the contralateral eye and triggers horizontal rotation of both eyes away from the stimulated eye (Collewijn 1975 ; Mustari & Fuchs 1990). Thus in order to drive eye rotation, monocular NT stimuli must activate the ipsilateral NOT by an indirect pathway, with information transferred back across the midline. The fact that NT stimuli inhibit the NOT (Hoffmann & Schoppmann 1975) and the presence of spontaneously active, likely GABAergic, neurons in the NOT which project to the contralateral NOT (Prochnow *et al.* 2007) suggests the hypothesis that NT stimuli activate the ipsilateral NOT by relieving reciprocal inhibition. Thus the reduced response of *twitch twice/robo3* mutants to NT stimuli would arise from defective midline crossing of the inhibitory connection.

The bilateral symmetry of the vertebrate brain plan imposes a need for robust lines of communication between the two sides of the brain. Our data show that the *robo3* gene plays an important role in establishing the commissural tracts that allow the two halves of the brain to distribute sensory stimuli and coordinate motor responses in a manner required for normal behavior.

Supplementary Material

Refer to Web version on PubMed Central for supplementary material.

Acknowledgements

This work was funded by a NRSA postdoctoral fellowship to H.A.B., National Institute of Health grant DK-069466 to S.L.J and National Institute of Health grants NS-048258 and MH-075691 to M.G.

References

Bashaw GJ, Kidd T, Murray D, Pawson T, Goodman CS. Repulsive axon guidance: Abelson and Enabled play opposing roles downstream of the roundabout receptor. Cell 2000;101:703–715. [PubMed: 10892742]

Beck JC, Gilland E, Tank DW, Baker R. Quantifying the ontogeny of optokinetic and vestibuloocular behaviors in zebrafish, medaka, and goldfish. J Neurophysiol 2004;92:3546–3561. [PubMed: 15269231]

Bosley TM, Salih MA, Jen JC, Lin DD, Oystreck D, Abu-Amero KK, MacDonald DB, al Zayed Z, al Dhalaan H, Kansu T, Stigsby B, Baloh RW. Neurologic features of horizontal gaze palsy and progressive scoliosis with mutations in ROBO3. Neurology 2005;64:1196–1203. [PubMed: 15824346]

Burgess H, Granato M. Modulation of locomotor activity in larval zebrafish during light adaptation. Journal of Experimental Biology 2007a;210:2526. [PubMed: 17601957]

Burgess H, Granato M. Sensorimotor Gating in Larval Zebrafish. Journal of Neuroscience 2007b; 27:4984. [PubMed: 17475807]

Camurri L, Mambetisaeva E, Davies D, Parnavelas J, Sundaresan V, Andrews W. Evidence for the existence of two Robo3 isoforms with divergent biochemical properties. Mol Cell Neurosci 2005;30:485–493. [PubMed: 16226035]

Challa AK, Beattie CE, Seeger MA. Identification and characterization of roundabout orthologs in zebrafish. Mech Dev 2001;101:249–253. [PubMed: 11231085]

Challa AK, McWhorter ML, Wang C, Seeger MA, Beattie CE. Robo3 isoforms have distinct roles during zebrafish development. Mech Dev 2005;122:1073–1086. [PubMed: 16129585]

Chen Z, Gore BB, Long H, Ma L, Tessier-Lavigne M. Alternative splicing of the Robo3 axon guidance receptor governs the midline switch from attraction to repulsion. Neuron 2008;58:325–332. [PubMed: 18466743]

Clark, DT. Visual Responses in Developing Zebrafish (Brachydanio rerio). Oregon; Eugene: 1981.

Collewijn H. Oculomotor areas in the rabbits midbrain and pretectum. J Neurobiol 1975;6:3–22. [PubMed: 1185174]

Dickson BJ. Molecular mechanisms of axon guidance. Science 2002;298:1959–1964. [PubMed: 12471249]

Douglas GR, Jiao J, Gingerich JD, Gossen JA, Soper LM. Temporal and Molecular Characteristics of Mutations Induced by Ethylnitrosourea in Germ Cells Isolated from Seminiferous Tubules and in Spermatozoa of lacZ Transgenic Mice. Proceedings of the National Academy of Sciences of the United States of America 1995;92:7485–7489. [PubMed: 7638217]

Dretakis EK, Kondoyannis PN. Congenital scoliosis associated with encephalopathy in five children of two families. J Bone Joint Surg Am 1974;56:1747–1750. [PubMed: 4434049]

Easter S, Nicola G. The development of vision in the zebrafish (Danio rerio). Developmental Biology 1997;180:646–663. [PubMed: 8954734]

Eaton R, Lavender W, Wieland C. Identification of Mauthner-initiated response patterns in goldfish: Evidence from simultaneous cinematography and electrophysiology. Journal of Comparative Physiology A: Sensory, Neural, and Behavioral Physiology 1981;144:521–531.

Faber, DS.; Korn, H. Electrophysiology of the Mauthner Cell:Basic Properties, Synaptic Mechanisms and Associated Networks.. In: Faber, DS.; Korn, H., editors. Neurobiology of the Mauthner Cell. Raven Press; New York: 1978.

Fricke C, Lee JS, Geiger-Rudolph S, Bonhoeffer F, Chien CB. astray, a zebrafish roundabout homolog required for retinal axon guidance. Science 2001;292:507–510. [PubMed: 11313496]

Granato M, van Eeden FJ, Schach U, Trowe T, Brand M, Furutani-Seiki M, Haffter P, Hammerschmidt M, Heisenberg CP, Jiang YJ, Kane DA, Kelsh RN, Mullins MC, Odenthal J, Nusslein-Volhard C. Genes controlling and mediating locomotion behavior of the zebrafish embryo and larva. Development 1996;123:399–413. [PubMed: 9007258]

Haller S, Wetzel SG, Lutschg J. Functional MRI, DTI and neurophysiology in horizontal gaze palsy with progressive scoliosis. Neuroradiology 2008;50:453–459. [PubMed: 18214457]

Harris LR, Lepore F, Guillemot JP. Abolition of optokinetic nystagmus in the cat. Science 1980;210:91–92. [PubMed: 7414325]

Hatta K. Role of the floor plate in axonal patterning in the zebrafish CNS. Neuron 1992;9:629–642. [PubMed: 1382472]

Hirata H, Saint-Amant L, Downes GB, Cui WW, Zhou W, Granato M, Kuwada JY. Zebrafish bandoneon mutants display behavioral defects due to a mutation in the glycine receptor beta-subunit. Proc Natl Acad Sci U S A 2005;102:8345–8350. [PubMed: 15928085]

Hoffmann KP, Schoppmann A. Retinal input to direction selective cells in the nucleus tractus opticus of the cat. Brain Research 1975;99:359–366. [PubMed: 1182552]

Huang YY, Neuhauss SCF. The optokinetic response in zebrafish and its applications. Frontiers in Bioscience 2008;13:1899–1916. [PubMed: 17981678]

Jen JC, Chan WM, Bosley TM, Wan J, Carr JR, Rub U, Shattuck D, Salamon G, Kudo LC, Ou J, Lin DD, Salih MA, Kansu T, Al Dhalaan H, Al Zayed Z, MacDonald DB, Stigsby B, Plaitakis A, Dretakis EK, et al. Mutations in a human ROBO gene disrupt hindbrain axon pathway crossing and morphogenesis. Science 2004;304:1509–1513. [PubMed: 15105459]

Kawakami K, Takeda H, Kawakami N, Kobayashi M, Matsuda N, Mishina M. A transposon-mediated gene trap approach identifies developmentally regulated genes in zebrafish. Dev Cell 2004;7:133–144. [PubMed: 15239961]

Kidd T, Brose K, Mitchell KJ, Fetter RD, Tessier-Lavigne M, Goodman CS, Tear G. Roundabout controls axon crossing of the CNS midline and defines a novel subfamily of evolutionarily conserved guidance receptors. Cell 1998;92:205–215. [PubMed: 9458045]

Kimmel C, Eaton R, Powell S. Decreased fast-start performance of zebrafish larvae lacking mauthner neurons. Journal of Comparative Physiology A 1980;140:343–350.

Lee JS, Ray R, Chien CB. Cloning and expression of three zebrafish roundabout homologs suggest roles in axon guidance and cell migration. Dev Dyn 2001;221:216–230. [PubMed: 11376489]

Liu KS, Fetcho JR. Laser ablations reveal functional relationships of segmental hindbrain neurons in zebrafish. Neuron 1999;23:325–335. [PubMed: 10399938]

Long H, Sabatier C, Ma L, Plump A, Yuan W, Ornitz DM, Tamada A, Murakami F, Goodman CS, Tessier-Lavigne M. Conserved roles for Slit and Robo proteins in midline commissural axon guidance. Neuron 2004;42:213–223. [PubMed: 15091338]

Lorent K, Liu KS, Fetcho JR, Granato M. The zebrafish space cadet gene controls axonal pathfinding of neurons that modulate fast turning movements. Development 2001;128:2131–2142. [PubMed: 11493534]

Mambetisaeva ET, Andrews W, Camurri L, Annan A, Sundaresan V. Robo family of proteins exhibit differential expression in mouse spinal cord and Robo-Slit interaction is required for midline crossing in vertebrate spinal cord. Dev Dyn 2005;233:41–51. [PubMed: 15768400]

Miyasaka N, Sato Y, Yeo SY, Hutson LD, Chien CB, Okamoto H, Yoshihara Y. Robo2 is required for establishment of a precise glomerular map in the zebrafish olfactory system. Development 2005;132:1283–1293. [PubMed: 15716341]

Miyashita T, Yeo SY, Hirate Y, Segawa H, Wada H, Little MH, Yamada T, Takahashi N, Okamoto H. PlexinA4 is necessary as a downstream target of Islet2 to mediate Slit signaling for promotion of sensory axon branching. Development 2004;131:3705–3715. [PubMed: 15229183]

Mustari MJ, Fuchs AF. Discharge patterns of neurons in the pretectal nucleus of the optic tract (NOT) in the behaving primate. Journal of Neurophysiology 1990;64:77–90. [PubMed: 2388076]

Neff MM, Turk E, Kalishman M. Web-based primer design for single nucleotide polymorphism analysis. Trends Genet 2002;18:613–615. [PubMed: 12446140]

Parinov S, Sevugan M, Ye D, Yang WC, Kumaran M, Sundaresan V. Analysis of flanking sequences from dissociation insertion lines: a database for reverse genetics in Arabidopsis. The Plant cell 1999;11:2263–2270. [PubMed: 10590156]

Park KW, Morrison CM, Sorensen LK, Jones CA, Rao Y, Chien CB, Wu JY, Urness LD, Li DY. Robo4 is a vascular-specific receptor that inhibits endothelial migration. Dev Biol 2003;261:251–267. [PubMed: 12941633]

Prochnow N, Lee P, Hall WC, Schmidt M. In vitro properties of neurons in the rat pretectal nucleus of the optic tract. J Neurophysiol 2007;97:3574–3584. [PubMed: 17344379]

Qian H, Zhu Y, Ramsey DJ, Chappell RL, Dowling JE, Ripps H. Directional asymmetries in the optokinetic response of larval zebrafish (Danio rerio). Zebrafish 2005;2:189–196. [PubMed: 18248193]

Rajagopalan S, Vivancos V, Nicolas E, Dickson BJ. Selecting a longitudinal pathway: Robo receptors specify the lateral position of axons in the Drosophila CNS. Cell 2000;103:1033–1045. [PubMed: 11163180]

Rick JM, Horschke I, Neuhauss SC. Optokinetic behavior is reversed in achiasmatic mutant zebrafish larvae. Curr Biol 2000;10:595–598. [PubMed: 10837226]

Rinner O, Rick JM, Neuhauss SC. Contrast sensitivity, spatial and temporal tuning of the larval zebrafish optokinetic response. Invest Ophthalmol Vis Sci 2005;46:137–142. [PubMed: 15623766]

Roeser T, Baier H. Visuomotor behaviors in larval zebrafish after GFP-guided laser ablation of the optic tectum. J Neurosci 2003;23:3726–3734. [PubMed: 12736343]

Rozen, S.; Skaletsky, H. Primer3 on the WWW for general users and for biologist programmers.. In: S, K.; S, M., editors. Bioinformatics Methods and Protocols: Methods in Molecular Biology. Vol. 132. Humana Press; Totowa, NJ: 2000. p. 365-386.

Sabatier C, Plump AS, Le M, Brose K, Tamada A, Murakami F, Lee EY, Tessier-Lavigne M. The divergent Robo family protein rig-1/Robo3 is a negative regulator of slit responsiveness required for midline crossing by commissural axons. Cell 2004;117:157–169. [PubMed: 15084255]

Sicotte NL, Salamon G, Shattuck DW, Hageman N, Rub U, Salamon N, Drain AE, Demer JL, Engle EC, Alger JR. Diffusion tensor MRI shows abnormal brainstem crossing fibers associated with ROBO3 mutations. Neurology 2006;67:519. [PubMed: 16894121]

Simpson JH, Kidd T, Bland KS, Goodman CS. Short-range and long-range guidance by slit and its Robo receptors. Robo and Robo2 play distinct roles in midline guidance. Neuron 2000;28:753–766. [PubMed: 11163264]

Stein E, Tessier-Lavigne M. Hierarchical organization of guidance receptors: silencing of netrin attraction by slit through a Robo/DCC receptor complex. Science 2001;291:1928–1938. [PubMed: 11239147]

Tessier-Lavigne M, Goodman CS. The molecular biology of axon guidance. Science 1996;274:1123–1133. [PubMed: 8895455]

Yasargil GM, Diamond J. Startle-response in teleost fish: an elementary circuit for neural discrimination. Nature 1968;220:241–243. [PubMed: 5303130]

Zottoli SJ, Newman BC, Rieff HI, Winters DC. Decrease in occurrence of fast startle responses after selective Mauthner cell ablation in goldfish (Carassius auratus). J Comp Physiol [A] 1999;184:207–218.

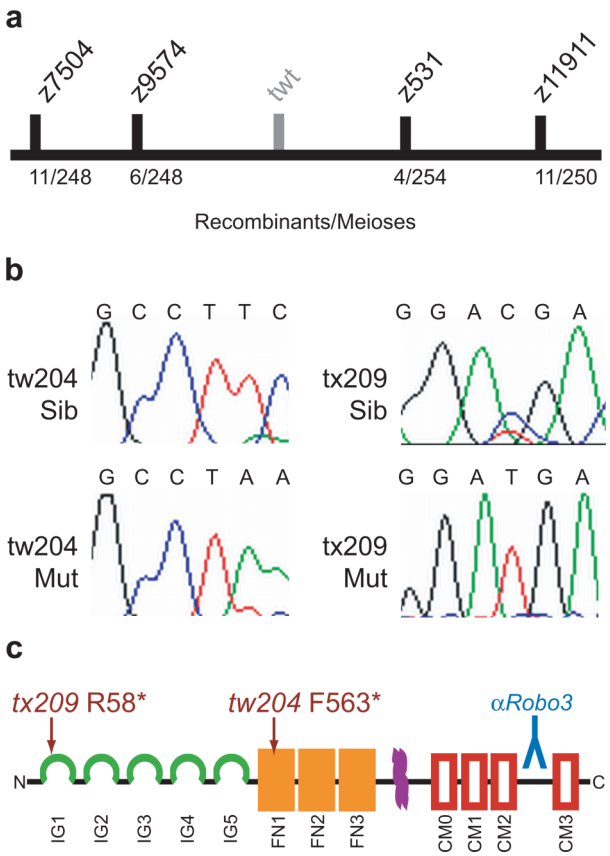

Figure 1. Positional Cloning and Sequence Analysis of *robo3*

(a) Recombination mapping placed *twitch twice* between Z-markers z9574 and z531 on linkage group 10. (b) Sequence analysis of cDNA from *robo3* demonstrated nonsense mutations in both the *tw204* and *tx209* alleles of *twitch twice*. (c) Domain structure of *robo3* showing the predicted truncated proteins generated by the mutations. The *tx209* allele is predicted to truncate *robo3* at amino acid R58 in the first immunoglobulin domain (green). The *tw204* allele truncates the protein at F563 in the first fibronectin domain (orange). Also shown is the transmembrane domain (purple), conserved roundabout motif boxes (red) and region used to make the antibody (blue).

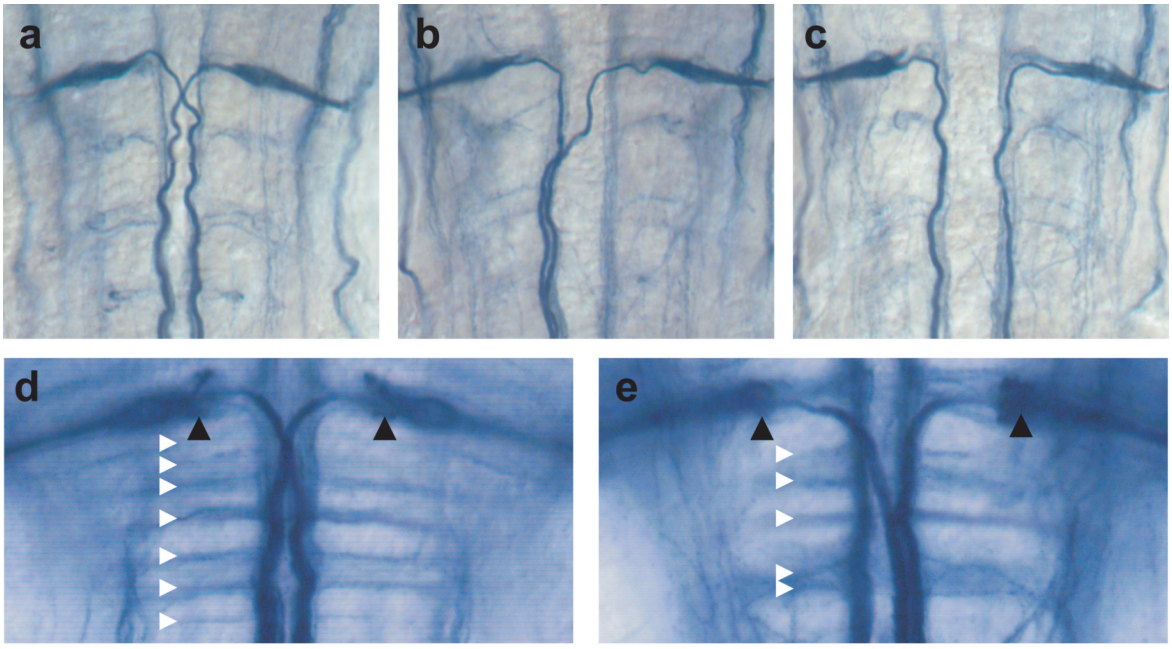

Figure 2. Mauthner axons fail to cross the midline in *twitch twice/robo3*

Immunostaining with the 3A10 antibody in 48 hpf embryos highlights the Mauthner cell and axons. In wildtype sibling embryos (a) both Mauthner axons cross the midline and project caudally. In *twitch twice/robo3* mutants (b,c) one or both Mauthner axons fail to cross the midline and project to ipsilateral spinal cord. At 6 dpf, immunostaining with the 3A10 antibody reveals a characteristic ladder of commissures (white triangles) and the axon cap of the Mauthner cell (black triangles) in wildtype larvae (d). Commissures are disorganized in *twitch twice/robo3* mutants although the Mauthner axon cap is intact (e).

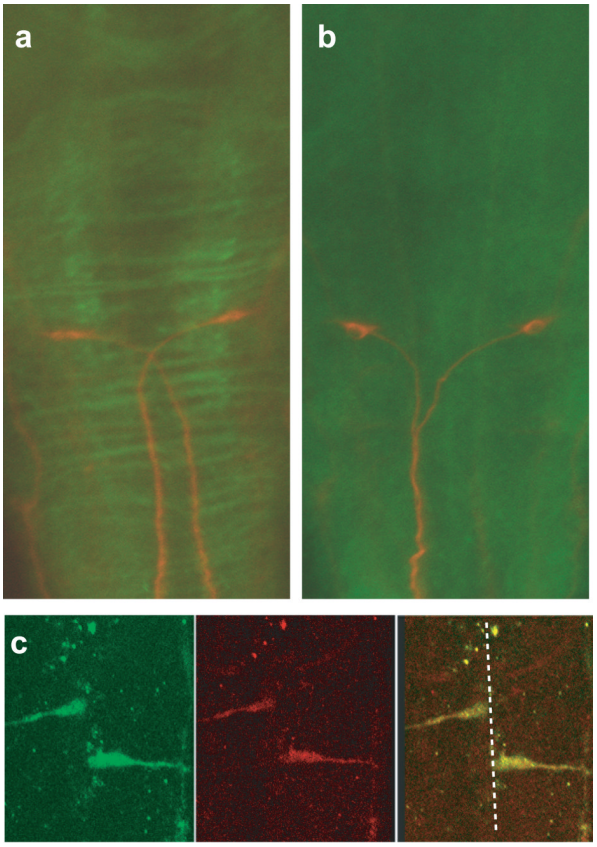

Figure 3. *robo3* is expressed in commissural axons

(a,b) Co-immunostaining of 48 hpf larvae was performed with anti-*robo3* (green) and the 3A10 antibody (red) to show the Mauthner axon phenotype in wild-type sibling larvae (a) and *twitch twice/robo3* mutants (b). (c) *robo3* expression in pre-crossing growth cones was analyzed by fixing actin:GFP transgenic fish at 10 minute intervals starting at 18 somites. Anti-GFP (green) and anti-*robo3* staining colocalize demonstrating that *robo3* is expressed before Mauthner axons have crossed the midline.

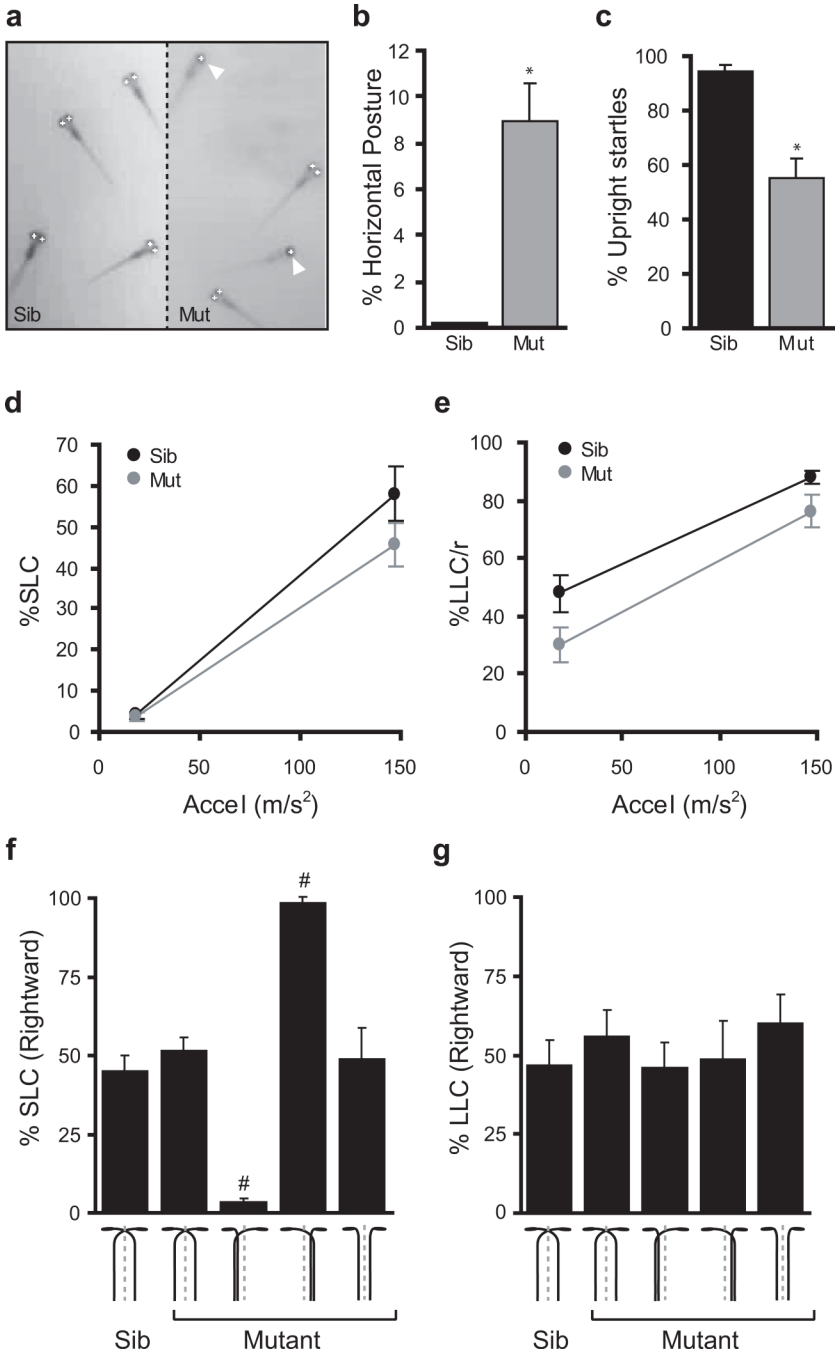

Figure 4. Startle responses are unidirectional in *twitch twice*/*robo3* mutants with Mauthner crossing defects

(a) Whereas wildtype sibling larvae remain vertically oriented in the water column, *twitch twice* mutants frequently lie on their side at the bottom of the dish and can be automatically recognized by the analysis software as only one eye is visible to the camera. (b) In stationary larvae, measuring the 'single eye' phenotype as a surrogate for horizontal posture shows that wildtype sibling fish very rarely adopt a horizontal posture, whereas *twt*^{tw204} mutant larvae frequently lie on their side indicating a balance defect (n=5 groups each). (c) *Twitch twice/robo3* mutants roll during startle responses. Wildtype sibling larvae remain vertically oriented for at least 90% of the recording window. Such responses are classified as 'Upright'. In contrast,

twt^{tw204} mutants show a strong tendency to roll during their startle response, with less than 60% of responses being categorized as Upright (n=5 groups each). (d) SLC startle responses to a series of 40 acoustic stimuli at two intensities (presented in a pseudorandom order) are elicited with similar frequency in sibling and *twt*^{tw204} mutants (n=5 groups each). (e) LLC startle responses are elicited with lower frequency in sibling and *twt*^{tw204} mutants. (f) SLC startle direction was assessed as the proportion of trials in which responses were initiated in a rightward direction. *twt*^{tw204} larvae were presorted according to Mauthner axon phenotype (schematically depicted, n=10 larvae each set) before testing. (g) LLC startle direction was assessed as for (f). * t-test $p < 0.01$; # one-sample t-test against 50% $p<0.001$.

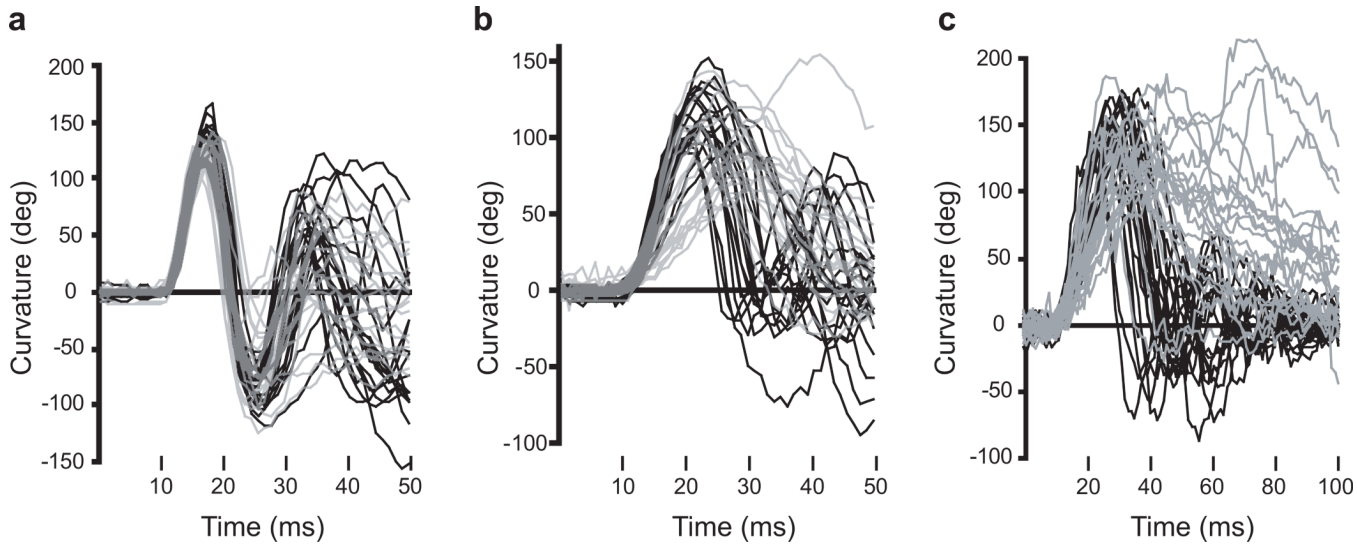

Figure 5.

C-Bend kinematics are disrupted in *twitch twice/robo3* mutant LLC and O-Bend responses. Larval curvature is plotted for wildtype sibling (black, n=18−20) and *twt*^{tw204} (grey, n=18−20) responses. Response latencies vary, so curves were manually inspected and shifted so that the beginning of each response is at the same position on the x-axis. For SLC (a) and LLC (b) responses to an acoustic stimulus, a 50 ms interval is shown, whereas a 100 ms interval is shown for the O-Bend response to a dark flash stimulus to accommodate the longer duration bend and counterbend (c).

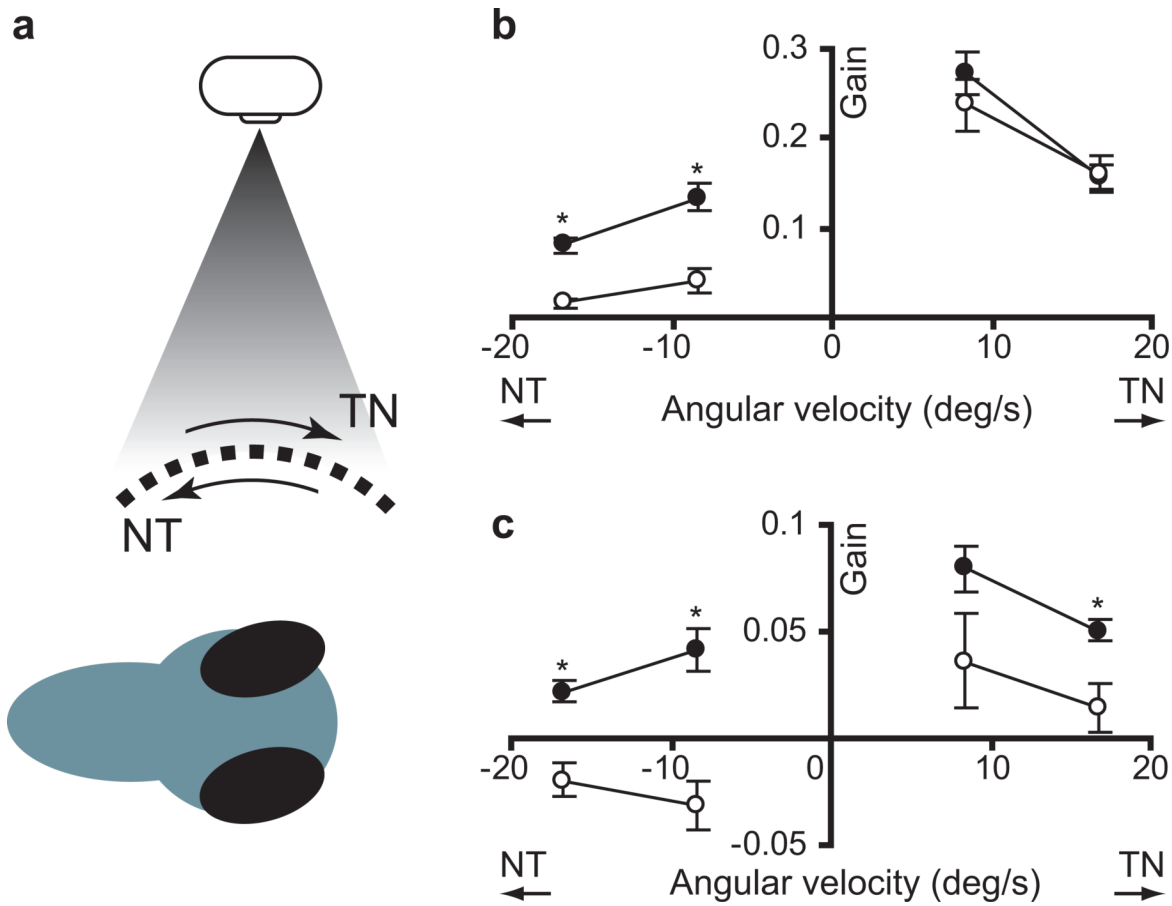

Figure 6. Horizontal eye movements in *twitch twice*/*robo3* mutants

(a) The optokinetic response was elicited by presenting a moving grating to one eye. Both the stimulated eye and the unstimulated eye rotate in the same direction as the stimulus. Angular velocity of eye movement in the stimulated eye (b) and unstimulated eye (c) was measured for low and high angular velocity stimuli for wildtype sibling (black, n=15) and *twt*^{tw204} mutant larvae (grey, n=15). Negative angular velocity trials represent the stimulus moving in a nasal to temporal direction, while positive angular velocity represents a temporal to nasal stimulus. * $p < 0.05$.

Table 1

stic startle and dark flash responses in *twitch twice/robo3*

duration and maximal angular velocity for the initial C-bend and counterbend are tabulated for sibling and oups of 20 larvae each). SLC and LLC responses were elicited using an acoustic stimulus, while O-Bends h.

	Initial C-Bend			Counterbend		
	Duration (ms)	**Max Ang Vel (°/ms)**	**Ang (°)**	**Duration (ms)**	**Max Ang Vel (°/ms)**	
	7.6 ± 0.1	26.6 ± 0.2	85.4 ± 1.9	9.5 ± 0.2	17.7 ± 0.4	
	7.9 ± 0.1	24.5 ± 0.7	86.7 ± 5.8	9.9 ± 0.4	18.0 ± 0.6	
	13.3 ± 0.3	12.3 ± 0.3	34.0 ± 1.8	10.1 ± 0.2	8.0 ± 0.3	
	18.3 ± 0.7	10.8 ± 0.6	18.7 ± 2.3	9.2 ± 0.7	5.4 ± 0.4	
	15.7 ± 0.5	19.5 ± 0.5	29.6 ± 1.3	18.5 ± 0.4	14.4 ± 0.4	
	22.5 ± 1.4	14.5 ± 1.0	18.9 ± 2.0	31.9 ± 4.9	10.4 ± 0.7	
9 ± 3.4						*
7 ± 3.7						*

Genes Brain Behav. Author manuscript; available in PMC 2009 September 25.